


Nondispersive evolution of the pump mode in down-conversion processes and in the presence of Kerr nonlinearity

I. F. Valtierra , M. B. Gaeta, and A. B. Klimov 

Departamento de Física, Universidad de Guadalajara, Revolución 1500, 44420, Guadalajara, Jal., México

 (Received 28 June 2023; revised 12 January 2024; accepted 28 February 2024; published 18 March 2024)

We show that the dynamics of appropriately designed initially uncorrelated states of a two-mode electromagnetic field exhibits a nondispersive long-time propagation of the strongly excited mode in the down-conversion regime and in the presence of a Kerr nonlinearity. The decoherence processes do not significantly affect the stability of the evolution of the excited mode. The structure of the initial states leading to a nonspreading evolution depends only on the parameters of the Hamiltonian and can be experimentally prepared and tested.

DOI: [10.1103/PhysRevA.109.033714](https://doi.org/10.1103/PhysRevA.109.033714)

I. INTRODUCTION

The self-interaction effect in Kerr media [1], ($\chi^{(3)}$ nonlinearity), and second harmonic generation or down conversion [2] (related to the $\chi^{(2)}$ nonlinearities) are probably the most emblematic quantum processes where the entire spectrum of nonclassical features have been predicted and observed [3]. The possibility of enhancing nonclassical effects such as squeezing, antibunching, entanglement, and so on in the propagation of electromagnetic fields in media where both $\chi^{(2)}$ and $\chi^{(3)}$ nonlinearities are present [4], has attracted significant attention due to the feasibility of experimental realizations in different physical systems [5–9]. Recent research in this area has largely focused on studying the superconducting traveling-wave parametric amplifiers [10–15], the analysis of signal propagation in metamaterials [16] and applications to quantum metrology and quantum synchronization [17,18]. These effects occur on relatively short times and can be explained from a semiclassical point of view [2,19–23]. The analysis of the long-time evolution requires, however, extensive numerical calculations in the case of large intensities of (effectively) interacting fields. Usually, the resonant second harmonic generation (SHG) in the presence of Kerr-like nonlinearity is scrutinized, especially in relation to the enhanced quantum noise suppression [3,24–26].

In this paper, we show there is an interesting quantum dynamic effect in the opposite regime of down-conversion with an added self-interaction. In particular, the evolution of certain factorized initial states exhibits a nondispersive behavior of the strongly excited mode, reflected in long-time shape preservation of the corresponding Husimi distribution. From the experimental perspective, one may observe that both the average photon number and the phase fluctuation of an initial strong coherent state, interacting with a specifically chosen state of a weak mode in a nonlinear medium, are maintained approximately constant for sufficiently long time in the presence of moderate losses. Such an unexpected result may help

to design nonspreading wave packets propagating in a highly nonlinear environment.

II. EFFECTIVE HAMILTONIAN

The effective interaction Hamiltonian that describes the propagation of the two-mode field in the presence of $\chi^{(2)}$ and $\chi^{(3)}$ nonlinearities is

$$\hat{H} = \zeta (\hat{a}^\dagger \hat{b}^2 + \hat{a} \hat{b}^{\dagger 2}) + \tilde{\chi} (\hat{a}^\dagger \hat{a})^2, \quad (1)$$

where \hat{a} (\hat{b}) and \hat{a}^\dagger (\hat{b}^\dagger) are the boson annihilation (creation) operators, ζ and $\tilde{\chi}$ are effective strengths of nonlinear intermode interaction and self-phase modulation, which are proportional to the $\chi^{(2)}$ and $\chi^{(3)}$ susceptibilities, respectively [26–29]. The dimensionless form of the Hamiltonian (1)

$$\hat{h} = \hat{H}/\zeta = \hat{a}^\dagger \hat{b}^2 + \hat{a} \hat{b}^{\dagger 2} + \chi (\hat{a}^\dagger \hat{a})^2, \quad (2)$$

includes a term representing the Kerr-type interaction $\sim (\hat{a}^\dagger \hat{a})^2$, entering with a small parameter $\chi = \tilde{\chi}/\zeta \ll 1$. In the regime of the initially highly excited a mode, $n_a = \langle \Psi(0) | \hat{n}_a | \Psi(0) \rangle \gg 1$, $\hat{n}_a = \hat{a}^\dagger \hat{a}$ and low-excited b mode, $n_b = \langle \Psi(0) | \hat{n}_b | \Psi(0) \rangle$, $\hat{n}_b = \hat{b}^\dagger \hat{b}$, the effect produced by the down-conversion process and the nonlinear self-modulation is comparable if $\chi n_a^{3/2} \sim 1$. In this regime [26,27] the evolution of the coupled modes significantly differs from the evolution in the absence of self-interaction. In particular, the relation between the photon numbers in the a and b modes is preserved in the course of the evolution $n_a(t) \gg n_b(t)$ since the depletion of the a mode is suppressed by the intensity-dependent Stark shift generated by the Kerr nonlinearity. Yet a pump a -mode field rapidly becomes correlated with the signal b -mode field. This is reflected in a rapid deformation of the a -mode Husimi Q function

$$\mathcal{Q}_a(\alpha|\tau) = {}_a \langle \alpha | \hat{\rho}_a(\tau) | \alpha \rangle_a / \pi, \quad (3)$$

where $\hat{\rho}_a(\tau) = \text{Tr}_b(|\Psi(\tau)\rangle\langle\Psi(\tau)|)$, $|\Psi(t)\rangle$ is the evolved state of the entire system, and $\tau = \zeta t$ is the dimensionless time. The $\mathcal{Q}_a(\alpha|\tau)$ function becomes significantly delocalized already for $\chi \tau_{\text{def}} \sim n_a^{-1-\epsilon}$, for an initially strong coherent state $|\sqrt{n_a}\rangle_a$, where the parameter $\epsilon > 0$ depends on the initial

*andrei.klimov@academicos.udg.mx

(weakly excited) b -mode state (see discussion below). For longer times, $\chi\tau \sim 1$ the a -mode distribution function splits into several pieces. Such phase-space evolution is typical for nonlinear systems [3]. We note that both nonlinear effects contribute to the distortion of the initial strong a -mode coherent state. However, the down-conversion and the self-modulation processes lead to the opposite signs of the intensity-dependent phase shift. Loosely speaking, these two nonlinear effects “bend” the phase-space distribution in opposite directions. This allows for a choice of specific initial states of the signal and pump fields to cancel the effect of competing nonlinearities, leading to a strong suppression of deformation of the wave packet for long times.

To determine the set of states evolving nondispersively we proceed with an approximate diagonalization of the Hamiltonian (2) in the a mode. Let us consider the following transformation [30]:

$$\hat{Q} = \exp(-i\hat{\phi}_a \hat{n}_b / 2), \quad [\hat{Q}^\dagger, \hat{Q}] = |0\rangle_a \langle 0| \otimes \hat{I}_b, \quad (4)$$

where $e^{i\hat{\phi}_a}$ is the phase operator of the a mode. The operator (4) is almost unitary on the states where the contribution of the vacuum is negligible as, e.g., strong coherent states. Applying the transformation (4) to the Hamiltonian (2) $\hat{h}_Q = \hat{Q} \hat{h} \hat{Q}^\dagger$ and expanding the transformed Hamiltonian \hat{h}_Q in inverse powers of the average photon number in the a mode we arrive at the following approximate expression, which is diagonal in the photon-number a -mode basis, $\hat{n}_a |n\rangle_a = n |n\rangle_a$ (see Appendix A)

$$\hat{h}_Q \approx \sqrt{\hat{n}_a + 1/2} (\hat{b}^2 + \hat{b}^{\dagger 2}) + \chi \hat{n}_a^2 - \chi \hat{n}_a \hat{n}_b, \quad (5)$$

where the term $\sim \chi n_b^2 \ll 1$ was neglected. The Hamiltonian (5) is quadratic on the signal-field operators and after application of a squeezing transformation in the b mode

$$\hat{h}_d \approx \hat{S}^\dagger(\eta) \hat{h}_Q \hat{S}(\eta), \quad (6)$$

$$\hat{S}(\eta) = e^{\eta(\hat{b}^2 - \hat{b}^{\dagger 2})/2}, \quad \eta \approx \chi \sqrt{n_a} / 4, \quad (7)$$

it is reduced to the following form:

$$\hat{h}_d = 2\sqrt{2 + 4\hat{n}_a - (\chi \hat{n}_a)^2} \hat{K}_1 + \frac{\chi \hat{n}_a}{2} + \chi \hat{n}_a^2, \quad (8)$$

where

$$\hat{K}_1 = (\hat{b}^2 + \hat{b}^{\dagger 2})/4. \quad (9)$$

Formally, the Hamiltonian (8) can be expanded in the eigenbasis $\{|k\rangle_b\}$ of the operator (9)

$$\hat{K}_1 |k\rangle_b = k |k\rangle_b, \quad (10)$$

in powers of the a -mode “fluctuation operator” $\Delta \hat{n}_a = \hat{n}_a - n_a$, according to

$$\hat{h}_d |k\rangle_b \approx (h_0 + h_1 \Delta \hat{n}_a + h_2 (\Delta \hat{n}_a)^2) |k\rangle_b, \quad (11)$$

where, for experimentally feasible values of the parameters of the system $\sqrt{n_a} \chi \ll 1$ [26,27],

$$h_0 \approx \frac{\chi n_a}{2} + \chi n_a^2 + 4\sqrt{n_a} k, \quad (12)$$

$$h_1 \approx 2\chi n_a + 2n_a^{-1/2} k, \quad (13)$$

$$h_2 \approx \chi - n_a^{-3/2} k / 2 \quad (14)$$

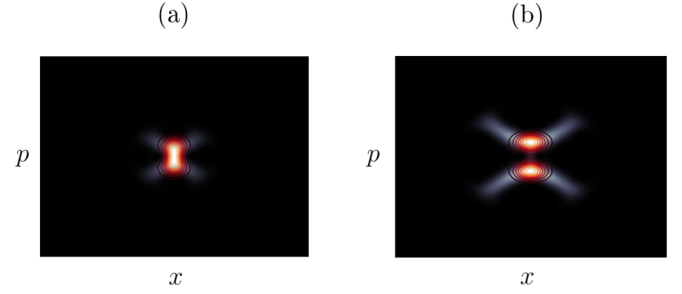


FIG. 1. Q functions of the b -mode states: (a) eigenstate of the \hat{K}_1 operator, $|k \approx 0.225\rangle$ (density plot) in comparison with the squeezed vacuum state (15) $|0; r = 0.406\rangle_b$ (contour plot); (b) eigenstate of the \hat{K}_1 operator, $|k \approx 0.957\rangle$ (density plot) in comparison with the squeezed cat state (17) $\sim |1.956i; r = -0.275\rangle_b + |-1.956i; r = -0.275\rangle_b$ (contour plot). Dark tones indicate low values of the Husimi Q function; the range of the dimensionless variables x and p is from -10 to 10 .

(exact expressions are given in Appendix A). Each component in the expansion (11) generates a specific type of evolution of an initial a -mode coherent state: the first term in (11) gives just to a global phase; the linear term $\sim \Delta \hat{n}_a$, leads to a rotation of the initial distribution around the origin in the field phase-space; the quadratic term $\sim (\Delta \hat{n}_a)^2$, produces an intensity-dependent phase shift and thus, a phase dispersion. One can observe from (14), that the down-conversion and Kerr processes give rise to the opposite dependence of phase shifts on the field intensity. This leads to a possibility of compensating the phase spreading.

It is worth noting that the elements of the basis $\{|k\rangle_b\}$ (10) are not normalizable, ${}_b \langle k' | k \rangle_b = \delta(k - k')$. However, some of the states $|k\rangle_b$ can be satisfactorily approximated by physical states of the quantum field. In particular, the scattering states $|k\rangle_b$, with $0 < k \lesssim 1$, are well approximated by squeezed vacuum states in the x direction with $n_b \lesssim 1$ (see Appendix B for a more precise estimation)

$$|k\rangle_b \approx |0; r\rangle_b = \hat{S}(r)|0\rangle_b, \quad (15)$$

$$r \approx 2k, \quad (16)$$

while for $k \gtrsim 1$, they can be fitted by squeezed cat-like states in the p direction with $n_b \gtrsim 1$,

$$|k\rangle_b \sim \hat{S}(-r)(|i\gamma\rangle_b + |-i\gamma\rangle_b), \quad (17)$$

$$2k \approx \gamma^2 e^{-2r}. \quad (18)$$

In Figs. 1(a) and 1(b) we plot the Q_b function for the b -mode states, where the density plots correspond to the exact eigenstates of \hat{K}_1 , and the contour plots were obtained using the following approximations: Fig. 1(a) $|k \approx 0.225\rangle$ and the corresponding squeezed vacuum state (15) with $r \approx 0.406$, $n_b = 0.174$; Fig. 1(b) $|k \approx 1.914\rangle$ and the squeezed cat state (17) with $r \approx 0.275$, $\gamma \approx 1.956$, $n_b \approx 2.32$.

III. FACTORIZED EVOLUTION

It follows from (14) and (16) that the coefficient h_2 of the nonlinear term $\sim (\Delta \hat{n}_a)^2$ in (11), which is responsible for the deformation of the wave packet, tends to zero in case of

low-excited b mode, $n_b \lesssim 1$ [corresponding to the Fig. 1(a)] if the following relation between the parameters of the system (χ, n_a) and the squeezing coefficient r (15) is fulfilled

$$r \sim 4\chi n_a^{3/2}. \quad (19)$$

Thus, the Hamiltonian (11) being applied to the squeezed b -mode states $|0; r = 4\chi n_a^{3/2}\rangle_b$ acquires the form

$$\hat{h}_d|0; r\rangle_b \approx (9\chi n_a^2 + \omega \Delta \hat{n}_a)|0; r\rangle_b, \quad \omega = 6\chi n_a. \quad (20)$$

Let us consider an initially strong a -mode coherent state $|\sqrt{n_a}\rangle_a$, $n_a \gg 1$, and an appropriately squeezed b -mode vacuum state

$$|\Psi(0)\rangle = \hat{Q}^\dagger \hat{S}^\dagger(\eta)|\sqrt{n_a}\rangle_a \otimes |0; r\rangle_b \quad (21)$$

$$\approx |\sqrt{n_a}\rangle_a \otimes \hat{S}(4\chi n_a^{3/2})|0\rangle_b, \quad (22)$$

where we use the property

$$\hat{Q}|\sqrt{n_a}e^{i\varphi}\rangle_a \approx e^{-i\varphi \hat{n}_a/2}|\sqrt{n_a}e^{i\varphi}\rangle_a + O(n_a^{-1/2}), \quad (23)$$

and the relation $\eta \ll r \lesssim 1$. Observe that the initial state for the signal field is determined by the pump mode state and the parameters of the Hamiltonian.

The evolution operator generated by the original Hamiltonian (2) has the following approximate form:

$$\begin{aligned} \hat{U}(\tau) &= e^{-i\hat{h}\tau} \\ &\approx \hat{Q}^\dagger \hat{S}^\dagger(\eta)e^{-i\tau \hat{h}_d} \hat{S}(\eta) \hat{Q}, \quad \tau = \zeta t. \end{aligned} \quad (24)$$

Then, taking into account (20), we notice that the evolved state (22) is kept approximately factorized, in the sense that one has (up to a global phase)

$$\begin{aligned} |\Psi(\tau)\rangle &= \hat{U}(\tau)|\Psi(0)\rangle \\ &\approx |e^{-i\omega\tau}\sqrt{n_a}\rangle_a \otimes |\psi(\tau)\rangle_b + O(n_a^{-1/2}), \\ |\psi(\tau)\rangle_b &= e^{-i\omega \hat{n}_b \tau/2}|0; 4\chi n_a^{3/2}\rangle_b. \end{aligned} \quad (25)$$

In other words, the a and b modes are approximately disentangled for a long time, up to $\chi\tau \sim n_a^{-1/2}$ in the course of the nonlinear evolution generated by (2), and both fields remain in nearly pure states during the interaction rather than in the mixed ones [see Fig. 4 in Appendix A where the evolution of the purity $P_a(\tau) = \text{Tr} \hat{\rho}_a^2(\tau)$ is plotted]. Then, the initial a -mode coherent state evolves nondispersively, just acquiring a time-dependent phase shift $\exp(-i\omega\tau)$. The corresponding \mathcal{Q}_a distribution rotates in the phase-space with basically no deformation

$$\mathcal{Q}_a(\alpha|\tau) \approx \mathcal{Q}_a(\alpha e^{-i\omega\tau}|0), \quad (26)$$

during several ($\sim \sqrt{n_a}$) periods of $T = 2\pi/\omega$. The timescale of the validity of the approximation (25), $\sqrt{n_a}\chi\tau \lesssim 1$ is restricted by the contribution of the terms $\sim (\Delta \hat{n}_a)^3$ in (11). The average number of photons in both modes remains constant in this approximation. It is worth noting that, in terms of the parameters of the b -mode field, the rotating frequency of the a -mode has the form $\omega \approx \frac{3}{4}n_a^{-1/2} \sinh 2r$.

In Fig. 2(a) we plot the exact (obtained from numeric simulations) evolution of the Q function of the a mode (represented as an orange blob) for the initial state (22) with $n_a = 83$, $\chi \approx 1.48 \times 10^{-4}$, so that $n_b \approx 0.173 = \text{const.}(t)$ and the period of rotation of the initial coherent-state distribution is $T \approx 84.7$

(in dimensionless units). One can observe that the \mathcal{Q}_a function rotates along the classical trajectory (dashed green line), $\alpha(\tau) = \alpha e^{-i\omega\tau}$, with practically no distortion during multiple periods, in complete accordance with the theoretical expression (26), where the predicted rotation frequency $\omega \approx 0.07396$ is very close to the numerical value $\omega_{\text{ex}} \approx 0.07412$.

The condition for nondispersive evolution when the b -mode contains an appreciable number of photons $n_b \gtrsim 1$, is $4\chi n_a^{3/2} \approx \gamma^2 e^{-2r}$ [corresponding to Fig. 1(b)] where γ is the amplitude of the cat-like state (17). The rotation frequency ω of the \mathcal{Q}_a distribution has the same functional form as for the squeezed vacuum state $\omega = 6\chi n_a$. However, the frequency ω depends in a different way on the characteristics of the b -mode state: $\omega \approx 3n_a^{-1/2}\gamma^2 e^{-2r}/2$. The numerical simulation of the evolution of the initial state (22) with the b mode prepared in the squeezed cat state (17), exhibits a similar behavior of the a -mode Q -function as in the case $n_b \lesssim 1$. In Fig. 2(d), we plot the exact evolution of the \mathcal{Q}_a function for the initial state

$$\begin{aligned} |\Psi(0)\rangle &= |\sqrt{n_a}\rangle_a \otimes \hat{S}(-\mu)(|i\gamma\rangle_b + |-i\gamma\rangle_b), \\ e^{2\mu} &= 4\chi n_a^{3/2}/\gamma^2, \end{aligned} \quad (27)$$

with $n_a = 83$, $\gamma \approx 1.956$, $\chi = 6.27 \times 10^{-4}$, where the period of rotation of the initial coherent-state distribution is $T \approx 20$. A different value of the coupling constant χ in the strong b -mode field is chosen for numerical convenience to restrict the effective dimension of the system. An experimental generation of Schrödinger cat states in optical waveguides was discussed in a recent paper [31].

When b -mode squeezing is absent, the modes rapidly become strongly correlated, leading to a significant distortion of the initial coherent state of the pump mode. In Fig. 2(c) the dynamics of \mathcal{Q}_a function for the initial states $|\sqrt{n_a}\rangle_a \otimes |0\rangle_b$ and $|\sqrt{n_a}\rangle_a \otimes (|i\gamma\rangle_b + |-i\gamma\rangle_b)$ are shown, where a quick deformation of the a -mode Q -function is clearly noted. We numerically determined the typical deformation time τ_{def} characterized by a relative phase-fluctuation in the pump mode

$$\delta^2(\tau_{\text{def}}) = \Delta^2 \Phi(\tau_{\text{def}})/\Delta^2 \Phi_{\text{CS}} \sim \lambda n_a^{1/2}, \quad (28)$$

$$\Delta^2 \Phi = \langle \cos^2 \hat{\phi}_a \rangle - \langle \cos \hat{\phi}_a \rangle^2, \quad (29)$$

where the initial coherent-state phase fluctuation is $\Delta^2 \Phi_{\text{CS}} \sim 1/2n_a$ and $\lambda \lesssim 1$ is a numerical factor. The deformation time is a small fraction of the period of rotation in both cases of a weak and intermediate b -mode field, with $\tau_{\text{def}} \sim T/n_a^{1/5}$ and $\tau_{\text{def}} \sim T/n_a^{2/5}$, respectively.

Thus, a relatively small squeezing of the signal vacuum or cat-state mode, for whose the squeezing parameter depends both on the interaction constants and the intensity of the pump mode, leads to a qualitatively different field dynamics.

IV. EXPERIMENTAL IMPLEMENTATION

It is worth noting that the initial states (22), leading to a nonspreading evolution, depend only on the parameters of the Hamiltonian and can be, in principle, prepared and experimentally tested. The effective interaction processes described by the Hamiltonian (2) can be implemented in optical systems with cascade second-order nonlinearities [32], nonlinear

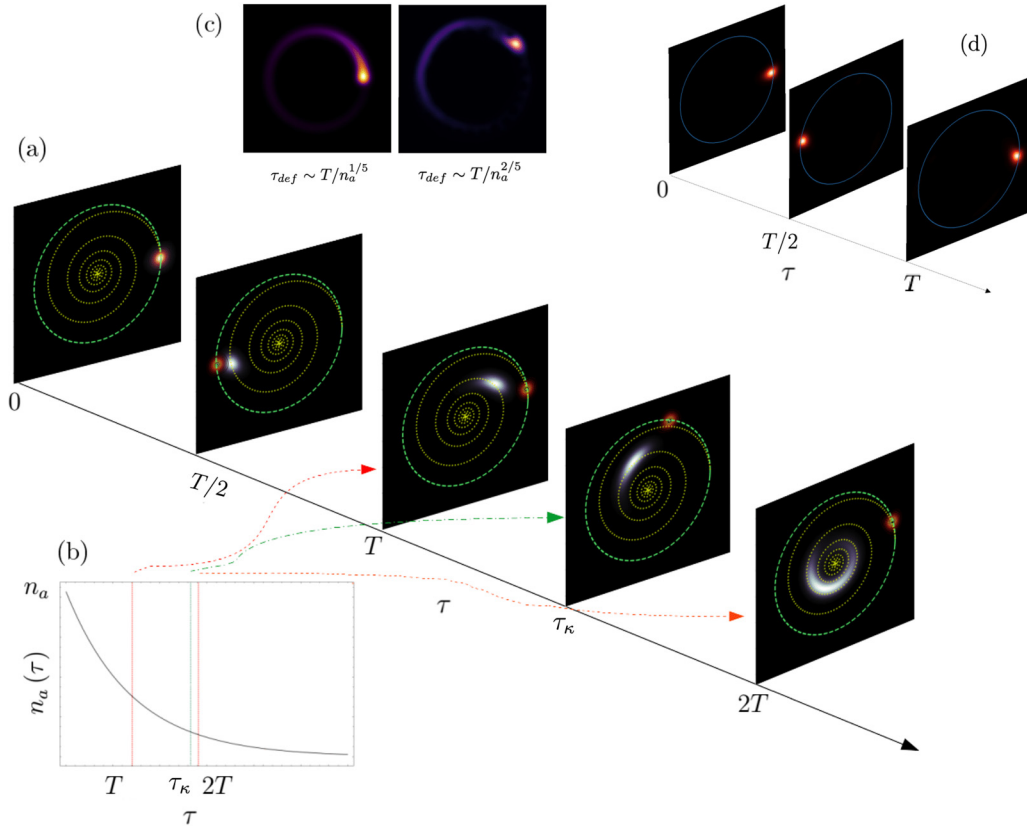


FIG. 2. (a) Snapshots of the phase-space evolution of the a -mode Q -function for the initial state (22) both in the absence (orange blob) and in the presence of dissipation (white blob) at some (dimensionless) time instances; $n_a = 83$, $\chi = 1.48 \times 10^{-4}$, $\kappa = 0.014$; the exact period of rotation in case of unitary evolution is $T = \pi n_a^{-1}/3\chi \approx 84.7$. (b) Evolution of the averaged photon number of the a -mode field in the presence of dissipation, $\kappa = 0.014$. (c) Left: Snapshot of the evolved a -mode Q -functions; Left: for the initial $|\sqrt{n_a}\rangle_a \otimes |0\rangle_b$, at $\tau_{\text{def}} \sim T/n_a^{1/5}\chi = 1.48 \times 10^{-4}$; Right: in the unitary phase-space evolution of the for the initial strong coherent a -mode state and the vacuum b -mode state, same values of n_a and χ ; Right: for the initial state $|\sqrt{n_a}\rangle_a \otimes (|i\gamma\rangle_b + |-i\gamma\rangle_b)$, $\chi = 6.27 \times 10^{-4}$, $\gamma \approx 1.956$ at $\tau_{\text{def}} \sim T/n_a^{2/5}$, $n_a = 83$ in both cases. (d) Snapshots of the phase-space unitary evolution of the a -mode Q -function for the initial state (27), $n_a = 83$, $\gamma \approx 1.956$, $\chi = 6.27 \times 10^{-4}$, where $T = \pi n_a^{-1}/3\chi \approx 20$ is the dimensionless period of rotation. In panels (a), (c), and (d), dark tones indicate low values of the Husimi Q function; the range of the dimensionless variables x and p is from -10 to 10 .

Fabry-Perot interferometers [33], Poled fibers [34], superconductive circuits [35,36], and so on [37].

A nondispersive propagation of a strong coherent state pump mode is achieved by injecting a squeezed vacuum signal mode according to Eq. (22). The squeezing parameter $r \approx 4\chi n_a^{3/2}$ is fixed as a function of the pump field intensity. For instance, for experimentally feasible susceptibilities $\chi^{(2)} \approx 9.45 \times 10^{-10}$ (m/V) and $\chi^{(3)} \approx 1.4 \times 10^{-13}$ (m/V)² [26,27], leading to the dimensionless coupling constant $\chi \sim 10^{-4}$ [27], and a coherent state with $n_a = 83$, the squeezing parameter is $r \approx 0.406$, which corresponds to a quantum noise squeezing ~ 3.5 dB. The nonspreading evolution of the pump-field wave packet is reflected in approximately constant average photon number and the phase fluctuations [38–40] in the case of small losses. The photon number preservation is clearly observed from the simulation of the Q_a -function dynamics, see Fig. 2(a), where the rotation radius $\sqrt{n_a(\tau)} \approx \text{const}(\tau)$.

Propagation of electromagnetic (EM) field pulses in nonlinear media is commonly accompanied by the phase noise increasing [41–44]. An interaction of a coherent state with a nonlinear environment leads to a quadrature squeezing for

times significantly shorter than the (quasi)period of motion. For longer times, the initial vacuum fluctuations are deformed in a complicated manner [45–50]. This affects the capacity for the transition of information codified in the phase variable [51]. Thus, a proposed scheme to cancel the phase fluctuation by modifying the initial state of the low-excited mode in the function of the coupling parameters and the strong field intensity can be helpful for designing weak fluctuating pulses, useful for carrying information in the phase variable. The effect of nondispersive propagation of the field in a nonlinear media can be experimentally verified by measuring the phase properties of the light pulse.

In Fig. 3 we plot the exact evolution of the a -mode phase fluctuation (29) for the initial squeezed b -mode vacuum (red solid line) and pure vacuum b -mode state (blue dashed line). A strong suppression of the phase fluctuation in case of the initial state (22) is evident. However, the large phase fluctuation for the initial vacuum state of signal mode is explained by a deformation of the initial a -mode field Q -distribution, as shown in Fig. 2(c).

It is worth noting that a very similar behavior of $\Delta^2\Phi$ is observed for an initial squeezed cat state [31] of the signal

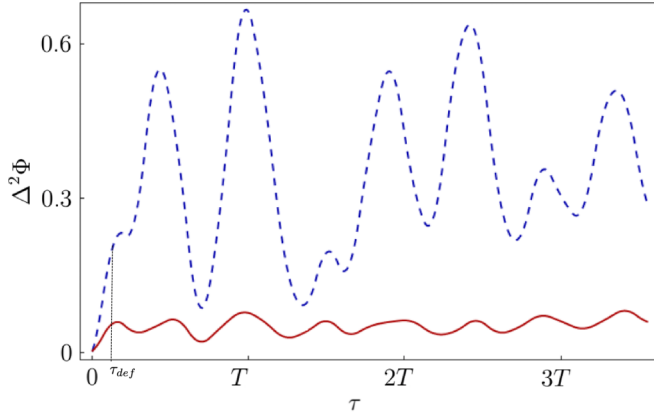


FIG. 3. Exact evolution of the a -mode phase fluctuation. Red solid line corresponds to the initial state (22) with $n_a = 83$, $r \approx 0.406$; blue dashed line corresponds to the initial state $|\sqrt{n_a}\rangle_a \otimes |0\rangle_b$; $\chi \approx 1.48 \times 10^{-4}$, the dimensionless period is $T = \pi n_a^{-1}/3\chi \approx 84.7$.

mode of the form (17) with $\gamma \approx 1.956$ and squeezing in the p direction $|r| \approx 0.275$ corresponding to -2.38 dB.

V. EFFECT OF DISSIPATION

A relevant feature of the factorized nondispersive evolution (25) is its relative stability, even in the presence of a strong a -mode dissipation. This follows from the transformation property of the (dimensionless) Lindblad equation

$$\begin{aligned} \partial_\tau \hat{\rho} &= -i[\hat{H}, \hat{\rho}] + \mathcal{L}\hat{\rho}, \\ \mathcal{L}\hat{\rho} &= \frac{\kappa}{2}(2\hat{a}\hat{\rho}\hat{a}^\dagger - \hat{a}^\dagger\hat{a}\hat{\rho} - \hat{\rho}\hat{a}^\dagger\hat{a}), \end{aligned} \quad (30)$$

under application of the \hat{Q} transformation (4),

$$\hat{Q}\mathcal{L}\hat{\rho}\hat{Q}^\dagger \approx \mathcal{L}\hat{\rho}_d + \Delta\mathcal{L}\hat{\rho}_d, \quad \hat{\rho}_d = \hat{Q}\hat{\rho}\hat{Q}^\dagger, \quad (31)$$

where $\|\Delta\mathcal{L}\hat{\rho}_d\| \sim O(\kappa n_b)$. Thus, the equation of motion for $\hat{\rho}_d$ is diagonal in the a -mode Hilbert space (in the leading approximation)

$$\partial_\tau \hat{\rho}_d \approx -i[\hat{h}_d, \hat{\rho}_d] + \mathcal{L}\hat{\rho}_d, \quad [\hat{h}_d, \mathcal{L}] = 0, \quad (32)$$

so the main dissipative effect consists only of the number of the a -mode photons. As a consequence, the initial state (22) evolves in the factorized form, where the purity of each mode is approximately preserved at the initial stages of the dissipative evolution

$$\hat{\rho}_d(\tau) \approx \hat{\rho}_a(\tau) \otimes \hat{\rho}_b(\tau) + O(n_a^{-1/2}(\tau)), \quad (33)$$

$$\hat{\rho}_a(\tau) = |e^{-i\omega\tau - \kappa\tau} \sqrt{n_a}\rangle_a \langle e^{-i\omega\tau - \kappa\tau} \sqrt{n_a}|, \quad (34)$$

$$\hat{\rho}_b(\tau) = |\psi(\tau)\rangle_b \langle \psi(\tau)|, \quad (35)$$

and the average number of the a -mode photons decays as $n_a(\tau) = n_a e^{-\kappa\tau}$, see Fig. 2(b). This leads to the shape preservation of the a -mode Husimi Q function, $\mathcal{Q}_a(\alpha|\tau) = \langle \alpha | \text{Tr}_b \hat{\rho}(\tau) | \alpha \rangle_a / \pi$, up to times where the approximation $n_a(\tau) \gg n_b$ holds. However, the corrections generated by the $\Delta\mathcal{L}\hat{\rho}_d$ term lead to a deformation of the rotating distribution for times $\tau_\kappa \sim (\kappa n_b)^{-1}$, as can be appreciated from

Fig. 2(a), where we plotted the exact dissipative evolution of the \mathcal{Q}_a function (white blob) with $\kappa = 0.014 \gg \chi \approx 1.48 \times 10^{-4}$. One can observe that the distribution evolves along the classical trajectory $\alpha(\tau) = e^{-i\omega\tau - \kappa\tau} \sqrt{n_a}$, approximately maintaining its shape despite the decrease in the photon number of the pump mode in accordance with (34).

VI. CONCLUDING REMARKS

We found that the propagation of an intense coherent pulse in the case of competing nonlinearities exhibits a nontrivial character if the initial conditions are appropriately matched with the parameters of the system: a strongly excited mode evolves nondispersively during a long time compared to the other timescales proper to the Hamiltonian (2) inclusively in the presence of a moderate dissipation. This type of dynamics results from the interplay of the Kerr and down-conversion nonlinearities that produce deformations in the “opposite directions” in the phase-space, allowing to mutually compensate them for an appropriately designed initial two-mode field. It is worth mentioning that the initial conditions for both fields are “tied” in the sense that the state of the b -mode “knows” the characteristics of the a -mode state, despite there being no direct initial correlation between them. In addition, the pump and the signal modes evolve independently for these special initial conditions, i.e., no intermode correlations are effectively generated for a long period of time.

Finally, such a mutual compensation of nonlinear effects can be used for stimulation of a nondispersive propagation of strong pulses of the pump mode in environments with $\chi^{(2)}$ and $\chi^{(3)}$ nonlinearities by appropriately designing the input signal field state.

APPENDIX A

In this Appendix, we deduce the effective Hamiltonian (A1)-(8) and the master equation (32). Applying the transformation (4) to the Hamiltonian (2) one obtains

$$\begin{aligned} \hat{h}_Q &= \hat{Q}\hat{h}\hat{Q}^\dagger \\ &= \hat{b}^2 \sqrt{\hat{n}_a - \hat{n}_b/2 + 1} + \sqrt{\hat{n}_a - \hat{n}_b/2 + 1} \hat{b}^{\dagger 2} \\ &\quad + \chi(\hat{n}_a - \hat{n}_b/2)^2. \end{aligned} \quad (A1)$$

Expanding the transformed Hamiltonian (A1) in the inverse powers of the average photon number in the a mode we arrive at the following approximate expression:

$$\hat{h}_d \approx \sqrt{\hat{n}_a + 1/2}(\hat{b}^2 + \hat{b}^{\dagger 2}) + \chi\hat{n}_a^2 - \chi\hat{n}_a\hat{n}_b. \quad (A2)$$

For highly excited a -mode initial states and in the limit $n_b \ll n_a$, where $n_a = \langle \Psi(0) | \hat{n}_a | \Psi(0) \rangle$, $n_b = \langle \Psi(0) | \hat{n}_b | \Psi(0) \rangle$, the Hamiltonian (A2) is approximated as follows:

$$\hat{h}_1 \approx \hat{h}_{11} + \frac{1}{\sqrt{\hat{n}_a + 1/2}} \hat{h}_{12} + O(n_a^{-1}), \quad (A3)$$

$$\hat{h}_{11} = \sqrt{\hat{n}_a + 1/2}(\hat{b}^2 + \hat{b}^{\dagger 2}) + \chi\hat{n}_a^2 - \chi\hat{n}_a\hat{n}_b, \quad (A4)$$

$$\hat{h}_{12} = -\frac{1}{8}\{\hat{n}_b, \hat{b}^{\dagger 2} + \hat{b}^2\}_+. \quad (A5)$$

The canonical transformation of the b -mode operators (7), diagonalizes the Hamiltonian (A4) in the Hilbert space of the

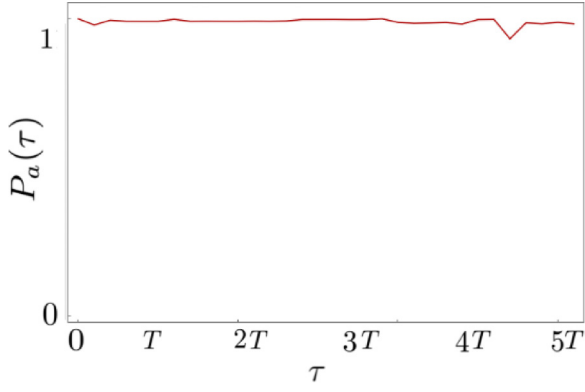


FIG. 4. The purity $P_a(\tau) = \text{Tr}\hat{\rho}_a^2(\tau)$ as a function of time in units of the dimensionless period of rotation of the a -mode Q -function $T = \pi/(3\chi n_a)$.

b mode (8) and the contribution of \hat{h}_{12} , with $\|\hat{h}_{12}\| \sim \chi(n_b + 1/2)^2$ is negligible in the limit $\chi n_b^2 \ll 1$.

Expanding the Hamiltonian (8) in powers of $\Delta\hat{n}_a = \hat{n}_a - n_a$, one obtains

$$\hat{h}_d \approx \hat{h}_0 + \hat{h}_1 \Delta\hat{n}_a + \hat{h}_2 (\Delta\hat{n}_a)^2 + \hat{h}_3 (\Delta\hat{n}_a)^3 + O(n_b/n_a), \quad (\text{A6})$$

where

$$\hat{h}_0 = \frac{\chi n_a}{2} + \chi n_a^2 + 2\sqrt{2 + 4n_a - (\chi n_a)^2} \hat{K}_1 \quad (\text{A7})$$

$$\hat{h}_1 = \frac{\chi}{2} + 2\chi n_a + \frac{2(2 - \chi^2 n_a) \hat{K}_1}{\sqrt{2 + 4n_a - (\chi n_a)^2}}, \quad (\text{A8})$$

$$\hat{h}_2 = \chi - \frac{2(2 + \chi^2) \hat{K}_1}{(2 + 4n_a - (\chi n_a)^2)^{3/2}}, \quad (\text{A9})$$

$$\hat{h}_3 = -\frac{2(2 + \chi^2)(n_a \chi^2 - 2) \hat{K}_1}{(2 + 4n_a - n_a^2 \chi^2)^{5/2}}. \quad (\text{A10})$$

In the limit $\sqrt{n_a} \chi \lesssim 1$ the expressions (A7) to (A9) acquire the form (12)–(14), in the basis $\{|k\rangle\}$ of the eigenstates of the operator (9) $\hat{K}_1|k\rangle = k|k\rangle$.

The coefficient \hat{h}_3 under the condition of absence of \hat{h}_2 (in the basis of eigenstates of \hat{K}_1) is restricted by $\|\hat{h}_3\| = O(kn_a^{-5/2})$. Thus, the last term in the expansion (A6) produces a sensible correction to the dynamics only for times $\chi\tau \gtrsim n_a/k$. For shorter times, $\chi\tau \sim n_a^{-1/2}$, the factorization (25) of the evolved initial state (22) is maintained. To inspect the precision of the factorization (25) in Fig. 4 we plot the exact evolution of the purity $P_a(\tau) = \text{Tr}\hat{\rho}_a^2(\tau)$. One can observe that the purity oscillates around unity during multiple periods of rotation of the a -mode distribution, $T = \pi/(3\chi n_a)$, confirming the validity of the approximations (22) to (25).

In the case of dissipative evolution the Q -transformed Lindblad operator, appearing in the master equation (30), takes the form (for initial strong a -mode states)

$$\hat{Q}\mathcal{L}\hat{\rho}\hat{Q}^\dagger \approx \mathcal{L}\hat{\rho}_d + \Delta\mathcal{L}\hat{\rho}_d, \quad (\text{A11})$$

where $\hat{\rho}_d = \hat{Q}\hat{\rho}\hat{Q}^\dagger$ and

$$\Delta\mathcal{L}\hat{\rho}_d = -\frac{\kappa}{4}(\hat{a}\{\hat{n}_b\hat{n}_a^{-1}, \hat{\rho}_d\}\hat{a}^\dagger - \hat{n}_b\hat{\rho}_d - \hat{\rho}_d\hat{n}_b), \quad (\text{A12})$$

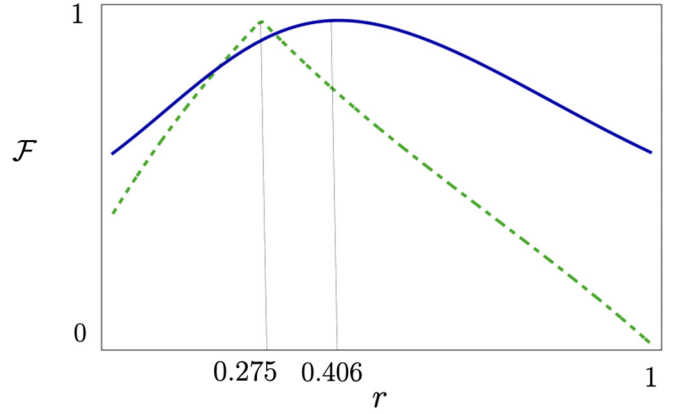


FIG. 5. The fidelity $\mathcal{F}(r) = |\langle k|0; r\rangle_b|^2$ blue solid curve, $k \approx 0.225$, and $\mathcal{F}(r) = |\langle k|\hat{S}(-r)(|i\gamma\rangle_b + |-i\gamma\rangle_b)|^2$, $k = 1.914$, $\gamma \approx 1.956$ green-dashed curve as functions of the squeezing parameter r .

which is restricted for highly excited a -mode coherent states by $\|\Delta\mathcal{L}\hat{\rho}_d\| \sim O(\kappa n_b)$.

APPENDIX B

The scattering eigenstates of a noncompact operator \hat{K}_1 , $\hat{K}_1|k\rangle = k|k\rangle$ can be approximated by physical states for small $k \ll 1$ and moderate $k \gtrsim 1$ eigenvalues.

In the case $k \ll 1$, in the approximation (15),

$$|k\rangle \approx |0; r\rangle = \hat{S}(r)|0\rangle, \quad (\text{B1})$$

the squeezing parameter is fixed by the condition

$$\langle 0; r|\hat{K}_1|0; r\rangle \approx k, \quad (\text{B2})$$

leading to the relation (16) between the parameters of the system

$$\sinh 2r \approx 4k, \quad (\text{B3})$$

so that $k \approx r/2$ for $k \lesssim 1$. The average number of the photons in this squeezed state (B1) to (B3) is $n_b = \sinh^2 r \lesssim 1$ and the fluctuation of \hat{K}_1 is approximately minimized. The overlap $\langle k|\hat{S}(r)|0\rangle$ can be analytically computed [52], and for $|k| \lesssim 1$ the following approximation for the fidelity is obtained

$$\mathcal{F}(r) = |\langle k|\hat{S}(r)|0\rangle|^2 \approx \frac{\pi|1 + (z_1 + z_2 k^2) \tanh r|^2}{4 \cosh r}, \quad (\text{B4})$$

where $z_1 \approx 0.3571 + 0.53511i$ and $z_2 = 0.36746 + 0.57219i$. In Fig. 5 the fidelity (B4) as a function of the squeezing parameter r of the squeezed vacuum state (15) and for the state $|k \approx 0.225\rangle$ shows the maximum at $r \approx 0.406$, which is consistent with (B3), here $n_b = 0.174$.

In the case $k \gtrsim 1$, the states $|k\rangle$ are approximated by squeezed cat-like states (17), where the condition (18), $2k \approx \gamma^2 e^{-2r}$, is obtained from the relation (B2), leading to the average number of photons

$$n_b \approx \sinh^2 r + \gamma^2 \text{sech}(\gamma^2) \sinh(\gamma^2 - 2r) \gtrsim 1.$$

The maximum of the fidelity $\mathcal{F}(r)$ for the squeezed cat state (17) and $|k = 1.914\rangle$ in Fig. 5 is achieved at $r \approx 0.275$, $\gamma \approx 1.956$, which is consistent with the approximation (18), here $n_b \approx 2.32$.

- [1] H.-H. Ritze and A. Bandilla, *Opt. Commun.* **29**, 126 (1979); R. Tanas and S. Kielich, *ibid.* **30**, 443 (1979); **45**, 351 (1983); G. J. Milburn and C. A. Holmes, *Phys. Rev. Lett.* **56**, 2237 (1986); S. Puri, S. Boutin, and A. Blais, *npj Quantum Inf.* **3**, 18 (2017); J.-J. Xue, K.-H. Yu, W.-X. Liu, X. Wang, and H.-R. Li, *New J. Phys.* **24**, 053015 (2022).
- [2] N. Bloembergen, *IEEE J. Sel. Top. Quantum Electron.* **6**, 876 (2000); M. Sukharev, A. Salomon, and J. Zyss, *J. Chem. Phys.* **154**, 244701 (2021); F. Mauger, P. M. Abanador, K. Lopata, K. J. Schafer, and M. B. Gaarde, *Phys. Rev. A* **93**, 043815 (2016).
- [3] M. Kozierowski and R. Tanas, *Opt. Commun.* **21**, 229 (1977); L.-A. Wu, H. J. Kimble, J. L. Hall, and H. Wu, *Phys. Rev. Lett.* **57**, 2520 (1986); G. Drobny and I. Jex, *Phys. Rev. A* **46**, 499 (1992); G. Drobny, I. Jex, and V. Bužek, *ibid.* **48**, 569 (1993); S. Nikitin and A. Masalov, *Quantum Opt.* **3**, 105 (1991); M. Lewenstein, M. Ciappina, E. Pisanty, J. Rivera-Dean, P. Stammer, T. Lamprou, and P. Tzallas, *Nat. Phys.* **17**, 1104 (2021), A. Goriach, O. Neufeld, N. Rivera, O. Cohen, and I. Kaminer, *Nat. Commun.* **11**, 4598 (2020).
- [4] N. Imoto, H. A. Haus, and Y. Yamamoto, *Phys. Rev. A* **32**, 2287 (1985).
- [5] R. E. Slusher, L. W. Hollberg, B. Yurke, J. C. Mertz, and J. F. Valley, *Phys. Rev. Lett.* **55**, 2409 (1985).
- [6] E. S. Polzik, J. Carri, and H. J. Kimble, *Phys. Rev. Lett.* **68**, 3020 (1992).
- [7] S. Schiller, G. Breitenbach, S. F. Pereira, T. Müller, and J. Mlynek, *Phys. Rev. Lett.* **77**, 2933 (1996).
- [8] K. Bergman, H. Haus, E. Ippen, and M. Shirasaki, *Opt. Lett.* **19**, 290 (1994).
- [9] S. F. Pereira, M. Xiao, H. J. Kimble, and J. L. Hall, *Phys. Rev. A* **38**, 4931 (1988).
- [10] B. Eom, P. Day, H. Leduc, and J. Zmuidzinas, *Nat. Phys.* **8**, 623 (2012).
- [11] M. T. Bell and A. Samolov, *Phys. Rev. Appl.* **4**, 024014 (2015).
- [12] M. Esposito, A. Ranadive, L. Planat, and N. Roch, *Appl. Phys. Lett.* **119**, 120501 (2021).
- [13] J. Heinsoo, C. K. Andersen, A. Remm, S. Krinner, T. Walter, Y. Salathé, S. Gasparinetti, J.-C. Besse, A. Potočnik, A. Wallraff *et al.*, *Phys. Rev. Appl.* **10**, 034040 (2018).
- [14] S. Kundu, N. Gheeraert, S. Hazra, T. Roy, K. V. Salunkhe, M. P. Patankar, and R. Vijay, *Appl. Phys. Lett.* **114**, 172601 (2019).
- [15] G. Burkard, M. J. Gullans, X. Mi, and J. R. Petta, *Nat. Rev. Phys.* **2**, 129 (2020).
- [16] A. Ranadive, M. Esposito, L. Planat, E. Bonet, C. Naud, O. Buisson, W. Guichard, and N. Roch, *Nat. Commun.* **13**, 1737 (2022).
- [17] D. Cui, J. Li, F. Li, Z.-C. Shi, and X. X. Yi, *Phys. Rev. A* **107**, 013709 (2023).
- [18] Y. Shen, H. Y. Soh, W. Fan, and L.-C. Kwek, *Phys. Rev. E* **108**, 024204 (2023).
- [19] Y.-R. Shen, *Principles of Nonlinear Optics* (Wiley-Interscience, New York, USA, 1984).
- [20] B. Jurco, *J. Math. Phys.* **30**, 1739 (1989).
- [21] D. F. Walls and R. Barakat, *Phys. Rev. A* **1**, 446 (1970).
- [22] J. Delgado, A. Luis, L. Sánchez-Soto, and A. Klimov, *J. Opt. B: Quantum Semiclass. Opt.* **2**, 33 (2000).
- [23] G. Alvarez and R. F. Alvarez-Estrada, *J. Phys. A: Math. Gen.* **28**, 5767 (1995).
- [24] L. Mandel, *Opt. Commun.* **42**, 437 (1982).
- [25] R. Tanaś and S. Kielich, *J. Mod. Opt.* **37**, 1935 (1990).
- [26] C. Cabrillo, J. L. Roldán, and P. García-Fernandez, *Phys. Rev. A* **56**, 5131 (1997).
- [27] N. T. Muradyan, *Opt. Commun.* **185**, 369 (2000).
- [28] M. Kitagawa and Y. Yamamoto, *Phys. Rev. A* **34**, 3974 (1986).
- [29] V. I. Kruglov and M. K. Olsen, *Phys. Rev. A* **64**, 053802 (2001).
- [30] A. Klimov and S. Chumakov, *Phys. Lett. A* **202**, 145 (1995).
- [31] W. S. Leong, M. Xin, Z. Chen, S. Chai, Y. Wang, and S.-Y. Lan, *Nat. Commun.* **11**, 5295 (2020).
- [32] A. White, J. Mlynek, and S. Schiller, *Europhys. Lett.* **35**, 425 (1996).
- [33] M. J. Collett and D. F. Walls, *Phys. Rev. A* **32**, 2887 (1985).
- [34] P. Kazansky, L. Dong, and P. S. J. Russell, *Opt. Lett.* **19**, 701 (1994).
- [35] Z. Leghtas, S. Touzard, I. M. Pop, A. Kou, B. Vlastakis, A. Petrenko, K. M. Sliwa, A. Narla, S. Shankar, M. J. Hatridge *et al.*, *Science* **347**, 853 (2015).
- [36] F.-X. Sun, Q. He, Q. Gong, R. Y. Teh, M. D. Reid, and P. D. Drummond, *Phys. Rev. A* **100**, 033827 (2019).
- [37] M. A. M. Marte, *Phys. Rev. Lett.* **74**, 4815 (1995).
- [38] G. I. Stegeman, M. Sheik-Bahae, E. Van Stryland, and G. Assanto, *Opt. Lett.* **18**, 13 (1993).
- [39] R. Tanas, T. Gantsog, and R. Zawodny, *Quantum Opt.* **3**, 221 (1991).
- [40] R. Lynch, *JOSA B* **4**, 1723 (1987).
- [41] T. Gantsog and R. Tanaś, *J. Mod. Opt.* **38**, 1537 (1991).
- [42] A. Luis, L. L. Sánchez-Soto, and R. Tanaś, *Phys. Rev. A* **51**, 1634 (1995).
- [43] J. Bajer, A. Miranowicz, and R. Tanaś, *Czech. J. Phys.* **52**, 1313 (2002).
- [44] L. Kunz, M. G. Paris, and K. Banaszek, *JOSA B* **35**, 214 (2018).
- [45] W. Vogel and W. Schleich, *Phys. Rev. A* **44**, 7642 (1991).
- [46] R. Lynch, *Phys. Rep.* **256**, 367 (1995).
- [47] D. T. Smithey, M. Beck, M. G. Raymer, and A. Faridani, *Phys. Rev. Lett.* **70**, 1244 (1993).
- [48] M. Raymer, D. Smithey, M. Beck, and J. Cooper, *Acta Phys. Pol. A* **86**, 71 (1994).
- [49] Z. Hradil, R. Myška, T. Opatrny, and J. Bajer, *Phys. Rev. A* **53**, 3738 (1996).
- [50] V. Belavkin, O. Hirota, and R. L. Hudson, *Quantum Communications and Measurement* (Springer Science & Business Media, New York, 2013).
- [51] L. G. Kazovsky, G. Kalogerakis, and W.-T. Shaw, *J. Lightwave Technol.* **24**, 4876 (2006).
- [52] M. M. Nieto and D. R. Truax, *Phys. Rev. Lett.* **71**, 2843 (1993).